

Mitigation of magnetic pollution generated by subsea cable on fish

Ilyes REZZAG BARA¹, Ahmed Nour El Islam AYAD¹, T. ROUIBAH¹, Wafa KRIKA²,
AYAD Abdelghani² and Salah-Eddine BENDIMERAD²

¹University Kasdi Merbah of Ouargla, Algeria

²University Djillali Liabes, Sidi Bel Abbes, Algeria

E-mail: rezzagbara.ilyes@univ-ouargla.dz

Abstract - Nowadays, The submarine power cables length increase gradually in the electrical network and produce very important electromagnetic fields emission. The electromagnetic field has an important harmful effect on the marine environment and species. The aim of this paper is to simulate the magnetic pollution produced by the high voltage altering current (HVAC) submarine power cable. The mathematical model of magnetic field calculation is used to show the magnetic flux density distribution around the power cable, the induced current on several fishes placed near the submarine cable. The marine species protection from electromagnetic pollution can be mitigated by several solutions as : shielding or burial depth. In our study the shielding is proposed as solution to reduce the magnetic pollution. The simulation results present the assessments of magnetic field in position and current variations in two cases before and after shielding. Finally, the simulation aim is to predict and minimize the biological and environmental harmful effects on marine animal species.

Keywords - Electric cable, Emission, Magnetic field, Mitigation, Shielding, Submarine.

I. INTRODUCTION

Many different shapes and styles of subsea power cables have been installed during more than hundred years. The number of subsea cables increase quickly in the electrical network and generate an important electromagnetic field (EMF) emissions and interactions with submarine species like fish [1,2]. Many works have studied the electromagnetic field characteristics, the interference, the effect of power, and the type of current HVDC or HVAC (direct or alternating current) [3,4].

This paper focuses here on Electromagnetic field emissions of three core submarine XLPE HVAC cable (cross-linked polyethylene, high-voltage alternating current 500 mm², 220 kV) near fish (magneto-receptive and electro-receptive species). Many researchers have studied the electromagnetic field characteristics, the interference, the effect of power, and the type of current HVDC or HVAC (direct or alternating current) [5,6]. The simulation results by COMSOL4.3 multiphysics with MATLAB

software show the magnetic field density distribution and intensities, around the different fish position in normal condition. Animal marine protection from electromagnetic emission can be used in the mitigation: by shielding or burial depth. In this paper mitigation is established and described.

II. THREE CORE SUBMARINE CABLE

HVAC submarine cables consist of copper or aluminum, depending on size and price. Cross-linked polyethylene (XLPE), with a maximum operating temperature of 90°C, is a commonly used insulation material [7].

A common construction of a three-core XLPE separate lead sheath-type submarine cable is shown in fig.1 with a frequency of 50 Hz, Rated current (Amplitude) $926 \cdot \sqrt{2}$ A Phase to ground voltage $220/\sqrt{3}$ kV where it contains[7]: (Fig. 1)

1:Conductor, 2:Conductor screen, 3:Insulation, 4:Insulation screening-semi conductive, 5:Screen, 6:Laminated sheath, 7:Optical fibers-optimally used for telecommunications, 8:Fillers, 9:Binder tapes

10: Armour Bedding-polypropylene strings,
11: Armor-galvanized round steel wires, 12: Serving
[7].

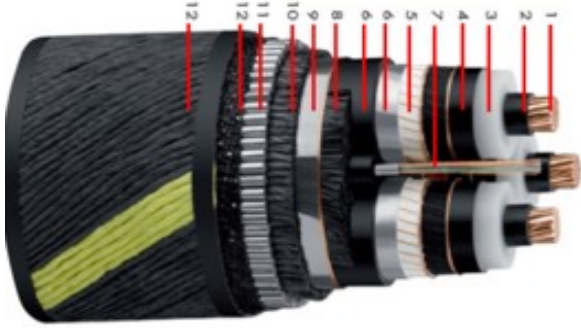


Fig. 1. Three core cable shape

III. MATERIALS DATA

Table 1 gives the structure sizes and characteristics of the cable. Table 2 presents the characteristics of different materials used in the model simulation for both single-core and three-core submarine electrical cables [7].

Table 1. Structure size of three-core XLPE cable [7].

Description	Value [mm]
Diameter of the conductor (Phase)	26.2
Insulation thickness (Phase)	24
Semi-conductive compound thickness (Phase)	0.85
Lead sheath thickness (Phase)	2.9
Diameter of fiber optic cable core	2.5
Armor thickness	6.5
The outer diameter of the cable	219
Diameter over insulation (Phase)	77.6
Diameter over phase (Phase)	89.2
Diameter over fiber optic core	2.5

Table 2. Materials characteristics of submarine power cables [7].

Materials	Electrical conductivity [S/m]	Relative permeability (per unit)	Relative permittivity (per unit)
Air	1·10 ⁻¹⁴	1	1
Polyethylene	1·10 ⁻¹⁸	1	2.25
Polypropylene	1·10 ⁻¹⁸	1	2.36
XLPE	1·10 ⁻¹⁸	1	2.5
Lead	4.55·10 ⁶	1	1
Copper	5.998·10 ⁷	1	1
High-strength alloy steel	4.032·10 ⁶	1	1
Semi-conductive compound	2	1	1
Silica glass	1·10 ⁻¹⁴	1	2.09
Sandy	1	1	28
Water	5.5·10 ⁻⁶	1	81

IV. CALCULATION OF THE MAGNETIC FIELD

The magnetic submarine cable study shows the field lines' distribution and magnitude at several positions. In theory, the resolution of the simulation model using differential or integrative equations depends on the condition and the properties of the problem of the device, solved by Maxwell's equations [7,8].

A) Maxwell's equation in variable regime

The four partials differentials Maxwell's equations explain the behavior of electromagnetic fields in the form of a mathematical model that employs proportional relationships related to the properties of materials and media, known as constitutive relations. The following equations represent Maxwell's law [9,10,11]:

$$\nabla \cdot D = \rho \quad (1)$$

$$\nabla \times E = - \frac{\partial B}{\partial t} \quad (2)$$

$$\nabla \cdot B = 0 \quad (3)$$

$$\nabla \times H = J' = J + J_D \quad (4)$$

Where: \vec{D} : the electric induction or electric displacement vector. ρ : the electric charge density

\vec{E} : the electric field vector

\vec{B} : the magnetic induction vector

\vec{H} : the Magnetic field vector

\vec{J}' : the electric current density

\vec{J} : the conduction current density

$\partial \vec{D} / \partial t$: the displacement current density.

The constitutive equation gave the relations between the fields by physical property in the subdomain:

$$B = \mu H = \mu_0 \mu_r H \quad (5)$$

$$J = \sigma E \quad (6)$$

Where : μ , μ_0 , μ_r : Permeability of the medium, vacuum, and relative respectively,

σ : Electrical conductivity.

B) Numerical Model

The model solves Maxwell-Ampere's law in 2D, using the out-of-plane magnetic vector potential A as a dependent variable [8]. All Maxwell's equations are either directly or indirectly involved together with

three constitutive relations and applied to the mathematical operation for establishing the final equation problem. We start with the combination of Gauss's and current conservation law. In the frequency domain, this gives:

$$\nabla \cdot (J + j\omega D) = 0 \quad (7)$$

When we replace the constitutive relations, we get the following equation:

$$\nabla \cdot (\sigma E + j\omega \varepsilon E) = 0 \quad (8)$$

The current density is defined by;

$J' = J + j\omega D$ is the sum of both conduction current and displacement current [8].

The second step of the model starts with Maxwell-Ampere's law; $\nabla \times H = J'$ then takes the divergence of that to get:

$$\nabla \cdot (\nabla \times H) = \nabla \cdot J' = \nabla \cdot (J + j\omega D) = 0 \quad (9)$$

We add the magnetic constitutive relation; $B = \mu H$

$$(\nabla \times H) = (\nabla \times (\mu^{-1} B)) = J' = (\sigma + j\omega \varepsilon) E \quad (10)$$

Next, let's consider the concept of a vector field A, the magnetic vector potential that is

$$\nabla \times A = B \quad (11)$$

And take the divergence

$$\nabla \cdot (\nabla \times A) = \nabla \cdot B = 0 \quad (12)$$

Maxwell's Faraday equation used for expressed E in terms of A [7, 8].

$$\nabla \times E = -j\omega B \quad (13)$$

$$\nabla \times E = -j\omega (\nabla \times A) = \nabla \times (-j\omega A) \quad (14)$$

$$E = -j\omega A \quad (15)$$

Now, both B and E are expressed in terms of A; if we substitute this result in (10), we will find:

$$\nabla \times (\mu^{-1} \nabla \times A) = (\sigma + j\omega \varepsilon) (-j\omega A) \quad (16)$$

Finally, if we swap some terms and put everything on the left side, we get the following 2D partial differential equation for the dependent variable A:

$$\nabla \times (\mu^{-1} \nabla \times A) - \omega^2 \varepsilon A + j\omega \sigma A = J_s \quad (17)$$

Where: J_s : the external current density

The magnetic fields interface uses this equation in the domains to determine the value of A and, consequently, the value of all fields derived from it [7, 8]. The input electric current of the three phases in time variation is as the following equations:

$$I_a = I_0, I_b = I_0 e^{-\frac{j2\pi}{3}}, I_c = I_0 e^{\frac{j2\pi}{3}} \quad (18)$$

V. GEOMETRIC AND CHARACTERISTICS

Figure 2 depicts the 2-D geometry for the numerical study composed by three-core, lead sheathed XLPE HVAC² submarine cable. It has a main conductor cross section of 500 mm², a phase-to-phase voltage of 220 kV, and carries a nominal current of 655 A and Fish body in front of the submarine cable both are submerged in water.

The study process is carried out on 3 different dimensions L1, L2 and L3 between the fish body and the submarine cable as in the figure 2.

Modeling of the fish body and submarine cable is in 2D, COMSOL software is used to carry out the simulation investigation, (the external boundary condition is of the Dirichlet type).

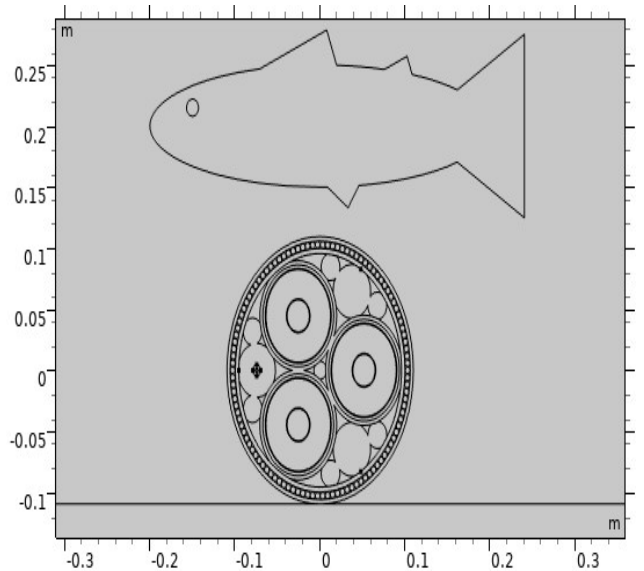


Fig. 2. Geometric characteristics of the model in 2D.

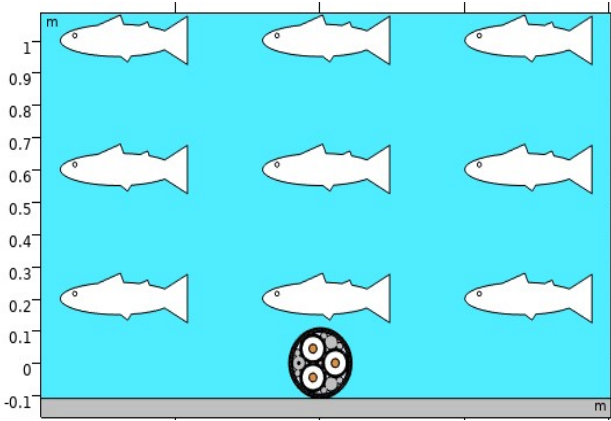


Fig. 3. Geometric of three different positions to fish body in 2D.

Table 3. Materials characteristics of fish [7].

	Relative permittivity (per unit)	Relative permeability (per unit)	Electrical conductivity [S/m]
Fish	17,7719E7	1	0,35

VI. SIMULATION RESULTS

The simulation results obtained the magnetic vector potential lines distribution with big concentration around the submarine cable is shown in figure 4.

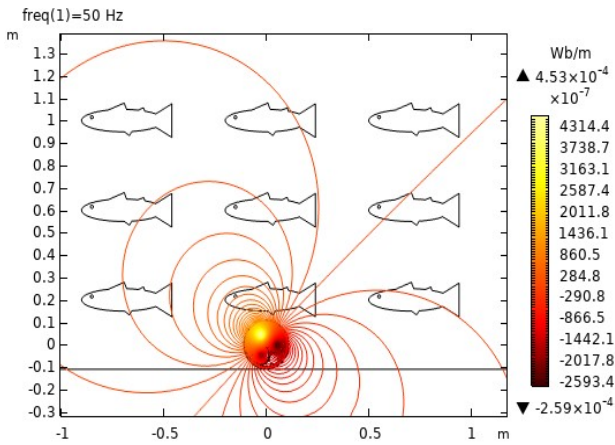


Fig. 4. Magnetic vector potential around the submarine cable.

The magnetic flux density value obtained is nearly above the lateral conductors. The important electrical current passed in the conductor produces a significant magnetic flux density around the cable surface. The density passes across the different cable layers to the outside. However, this concentration decreases as one move away from underground cables.

Table 4. Results of the magnetic flux density and in terms of different distances between the cable and fish.

The magnetic flux density (μT)			
Current	80%		
Position Fish	X=0m	X=0.7m	X=-0.7m
Y1=0.2m	620	27.4	25.22
Y2=0.6m	44.73	17.44	16.58
Y3=1m	15.05	9.84	9.6
Current	100%		
Position Fish	X=0m	X=0.7m	X=-0.7m
Y1=0.2m	775	34.25	31.5
Y2=0.6m	56	21.8	20.732
Y3=1m	18.7	12.3	12
Current	120%		
Position Fish	X=0m	X=0.7m	X=-0.7m
Y1=0.2m	930	41.09	37.82
Y2=0.6m	67.1	26.162	24.87
Y3=1m	22.57	14.764	14.4

Table 4 shows the magnetic flux density with load variation in the different position of fish produced by the subsea cable. (The maximum density is above the cable position with a load of 120% and X = 0m).

Mitigation of Magnetic Field by Shielding :

The electric transmission lines and distribution networks generate an important low-frequency magnetic field, which greatly necessitates the development of magnetic field mitigation procedures by minimizing the intensities in the sensitive zone with the shield technique. The technique is based on placing an additional mitigation system (conductive passive shield with an aluminum thickness of 4 mm), close to the source of the protected region.

Figure 4 reveals the conductive passive shield position near the three core submarine cables, and the magnetic lines are encircled between the aluminum and cables.

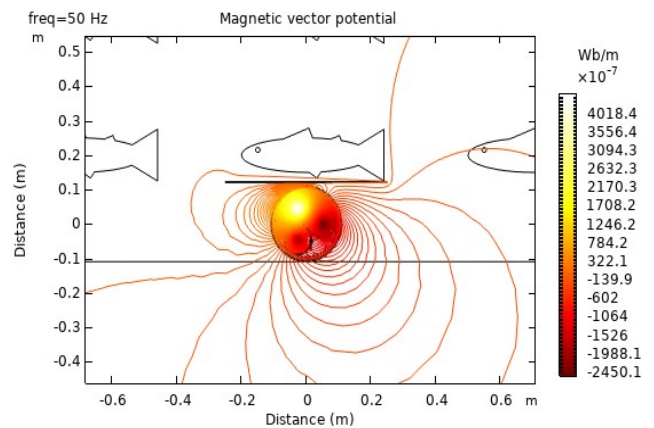


Fig. 5. Magnetic vector potential around the submarine cable after shielding.

The simulation results obtained the magnetic vector potential lines distribution after shielding distribution with a little bit concentration around the submarine cable compared to before shielding as shown in figure 6, 7 and table 5.

The passive shielding reduces the magnetic flux density aggression and emission near the fish.

Table 5. Results of the magnetic flux density and in terms of different distances between the cable and fish before and after shielding.

Shielding case	The magnetic flux density (μT)					
	Before shielding			After shielding		
Position	X=	X=	X=-	X=0m	X=	X=-
Fish	0m	0.7m	0.7m	0.7m	0.7m	0.7m
Y1=0.2m	775	775	34.25	21.82	14.505	21.37
Y2=0.6m	56	56	21.8	8.008	6.486	9.88
Y3=1m	18.7	18.7	12.3	3.645	3.491	5.22

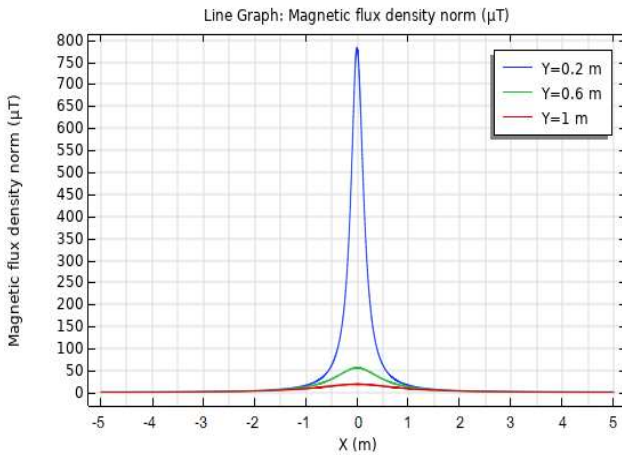


Fig. 6. Magnetic flux density and in terms of different distances before shielding

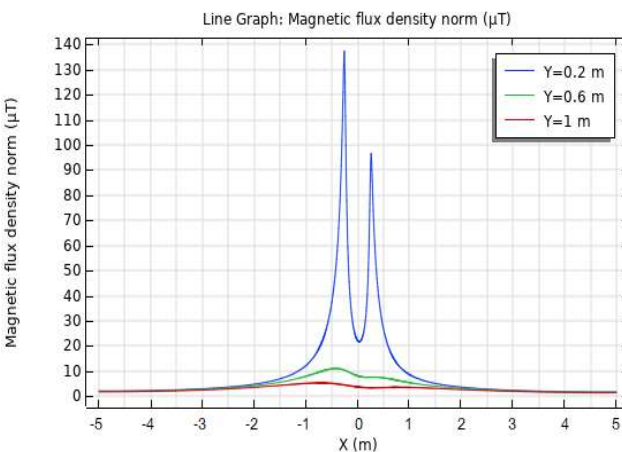


Fig. 7. Magnetic flux density and in terms of different distances after shielding.

VII. CONCLUSION

In this paper, we presented the finite element analysis of magnetic fields emitted by submarine

high-voltage power cables using COMSOL Multiphysics 5.4 and Matlab software. According to the simulation results, it can be drawn that the magnetic field lines have a greater concentration near the three-core submarine power cable, mainly with significant electrical current or load, but a decrease in function of far distance. From this investigation, it is noticed that the passive shielding has a very important effect on magnetic field emission reduction.

VIII. REFERENCES

- [1] G. Pedrazzoli and G. Rinzo, "HVAC Cable Systems," 2018 IEEE International Conference on Environment and Electrical Engineering and 2018 IEEE Industrial and Commercial Power Systems Europe (EEEIC / I&CPS Europe), Palermo, Italy, 2018, pp. 1-6.
- [2] B. Taormina et al., "A review of potential impacts of submarine power cables on the marine environment: Knowledge gaps, recommendations and future directions," *Renewable and Sustainable Energy Reviews*, vol. 96, no. 7, pp. 380-391, July 2018.
- [3] I. Jurdana, R. Ivčič and D. Glažar, "Submarine optical cables: Impact on the marine environment," *Proceedings ELMAR-2014*, Zadar, Croatia, 2014, pp. 1-4.
- [4] Y. Guo et al., "The Review of Electromagnetic Pollution in High voltage Power Systems," 3rd International Conference on Biomedical Engineering and Informatics (IEEE BMEI 2010), Yantai, China, 2010, pp 1322-1326.
- [5] S. Vaideki et al., "field analysis of high voltage submarine cables," 2017 International Conference on Computation of Power, Energy Information and Communication (ICCPEIC), Melmaruvathur, India, 2017, pp. 778-782.
- [6] K. Jayasinghe, "Power loss evaluation of submarine cables in 500MW offshore wind farm master of science," Ph.D. dissertation, department of earth sciences, uppsala university, Campus Gotland 2017.
- [7] W. Krika, A.N.E Ayad, L. Benyekhlef, F. Benhamida, "Electromagnetic simulation of subsea power cable pollution," International black sea coastline countries scientific research symposium VI, Giresun, Turkey, April 2021.
- [8] A. N. E. I. Ayad, W. Krika, H. Boudjella, A. Horch, "Simulation of the electromagnetic field in the vicinity of the overhead power transmission line," *European journal of Electrical Engineering*, vol. 21, no. 1, pp. 49-53, 2019, doi: 10.18280/ejee.210108.
- [9] W. Krika, A.N.E Ayad, L. Benyekhlef, F. Benhamida "Thermal effect of harmonic and short circuit in underground electric cable," International black sea coastline countries scientific research symposium VI, Giresun, Turkey, April 2021.